Complex Quasi-Two-Dimensional Crystalline Order Embedded in VO_{2} and Other Crystals

Timothy Lovorn and Sanjoy K. Sarker

Phys. Rev. Lett. **119**, 045501 — Published 27 July 2017

DOI: 10.1103/PhysRevLett.119.045501

Complex quasi two-dimensional crystalline order embedded in VO_2 and other crystals

Timothy Lovorn[1,2] and Sanjoy K. Sarker[1]

[1] *Department of Physics and Astronomy, The University of Alabama, Tuscaloosa, Alabama 35487, USA*
[2] *Department of Physics, The University of Texas at Austin, Austin, Texas 78712, USA*

Metal oxides such as VO_2 undergo structural transitions to low-symmetry phases characterized by intricate crystalline order, accompanied by rich electronic behavior. We derive a minimal ionic Hamiltonian based on symmetry and local energetics which describes structural transitions involving all four observed phases, in the correct order. An exact analysis shows that complexity results from the symmetry-induced constraints of the parent phase which forces ionic displacements to form multiple interpenetrating groups using low-dimensional pathways and distant neighbors. Displacements within each group exhibit independent, quasi two-dimensional order, which is frustrated and fragile. This selective ordering mechanism is not restricted to VO_2: it applies to other oxides which show similar complex order.

Introduction.—Vanadium dioxide (VO_2) undergoes a transition from a high-symmetry rutile structure to a lower-symmetry monoclinic M1 phase, with intricate antiferroelectric (AFE) crystalline order [1–4]. The lowering of symmetry doubles the unit cell, changing the electronic band structure and converting a metal into a dimerized Mott insulator which shows unusual metal-insulator coexistence near T_c. The insulating phase is structurally soft, as two other variants appear with doping or application of strain [5–8]. Although such materials are promising for applications (including low-dissipation logic [9–11] and many others), the lack of a microscopic theory has hindered progress. VO_2 is not alone: similar complex ordering also occurs in many other crystals [12–15], exhibiting diverse electronic and magnetic phases [16] whose properties would certainly reflect the intricacies of the underlying crystalline order. To understand exactly how this complexity appears and its effect on finite temperature properties, one needs a dynamical model to describe the structural phases.

In this Letter, we focus on VO_2 and derive a minimal Hamiltonian in terms of discrete ionic displacements based on the symmetry of the parent rutile (R) structure and local energetics. We find that the model has a broadly applicable selective ordering mechanism which is responsible for the complexity, which also leads to fragile quasi low-dimensional order embedded in the 3D system, features that were not known previously. In the R phase of VO_2, V ions occupy the sites of a body-centered tetragonal lattice surrounded by O octahedra. Below a temperature T_c (341 K) a monoclinic (M1) phase emerges in which V ions are slightly displaced to form dimers, which also twist, creating zigzag chains along the c-axis and giving rise to long-range AFE order. Another monoclinic phase (M2) and a triclinic one (T) are realized by modest doping or strain. In the M2 phase only one half of the V chains dimerizes, while the other half twists, leading to a different electronic behavior. Rice *et. al.* argued that dimerization in one chain induces a twist in a neighboring chain and that the M1 phase is a superposition of two M2 structures [17]. Phenomenological Landau theories based on two order parameters have been developed [18, 19] and applied close to the transition [20].

We show by a detailed mean-field analysis that the microscopic model, which is exactly mapped into a spin-1 two-component Ising (Ashkin-Teller [21, 22]) model, describes these complex phases. Further (exact) analysis reveals new features: the complex ordering is quasi two-dimensional, frustrated and fragile. These arise due to constraints imposed by the already ordered and densely packed parent (rutile) phase; the ions make intricate lower-energy displacements which order separately in several interpenetrating groups involving planes and distant neighbors. Neighbors belonging to different groups compete, creating local configurations which tend to frustrate order. This mechanism is also applicable to other systems showing similar complex order.

Ionic model.—To derive the model, we assume that the potential energy seen by a V ion at a site i has local minima along the c-axis and apical directions (in the ab-plane) located by displacement vectors $\mathbf{u}_i$, corresponding to its equilibrium positions in the rutile ($\mathbf{u}_i = 0$) and monoclinic phases ($\mathbf{u}_i \neq 0$). We construct a Hamiltonian in terms of $\mathbf{u}_i$, based on the symmetries of the rutile lattice and local energetics. This is an effective model since only V ions are considered; $\mathbf{u}$'s should be thought of as block variables describing displacements of V ions screened by the surrounding O ions and electrons.

The rutile phase has an *orientational order* which plays the central role in determining the Hamiltonian. The oxygen octahedra have two different orientations connected by a screw operation. Four O ions form a V-centered rectangle, with one side along the c-axis and the other on the ab-planes along one of the diagonals. All body center V ions have rectangles oriented one way, along [110], as shown in Fig. 1(a). All corner V ions have them in a perpendicular direction, along $[1\bar{1}0]$, as shown in Fig. 1(b). We denote the sets of planes in which these rectangles lie as A and B, respectively.

Consider a body-center V ion. The two O^{2-} ions below it lie along the diagonal of the ab-plane joining two corner V^{4+} ions. The effective V-O attraction is clearly the

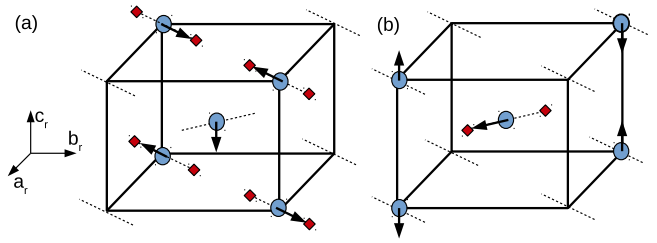

FIG. 1. Interaction between corner and body-center V ions. (a) Interaction between V ions (circles) along the [110] direction, mediated by corner site apical oxygens (diamonds). Corner V atom arrows point towards the low-energy displacement, assuming the indicated displacement of the body-center V atom. The rutile lattice vectors $\mathbf{a}_r$, $\mathbf{b}_r$, $\mathbf{c}_r$ are shown for reference. (b) Corresponding interaction between V ions along the $[1\bar{1}0]$ direction, mediated by body-center site apical oxygens.

strongest in this configuration; the minima for corner V ions, if they exist, will be along this line. Therefore, $\mathbf{u}$ has only one component, u_{ab}, in the ab-plane. There are no O ions, and hence no minima, along the other diagonal. When the two O ions move away from each other, they pull the two corner V ions along the ab-diagonal toward each other and push the two body-center V ions above and below away from each other vertically (by electrostatics). Hence, $\mathbf{u}$ has another component u_c along the c-axis. Thus, a twist (by u_{ab}) causes an out-of-phase dimerization (by u_c) via an interaction mediated by the O-pair (and O-V bonding electrons), as observed.

Each component has 3 values by mirror symmetry, and thus can be represented by a (pseudo) spin-1 Ising variable: $u_{ic} = u_z S_i$, $u_{iab} = u_x \sigma_i$, where S and σ take values $(0, \pm 1)$; u_x and u_z are positive (we use the convention $u_{iab} > 0$ when moving in the $+\hat{x}$ ($\mathbf{a}_r$) direction from site i). Thus we have an important result: structural transitions are described by a spin-1 two-component Ising (Ashkin-Teller) model. The rich critical properties exhibited by the spin-1/2 Ashkin-Teller model have been extensively studied. With 9 on-site states the spin-1 model can describe much more complex behavior [23, 24], but it has not been studied widely. Its realization in VO_2 and other crystals reflects the potential complexity of the latter's behavior.

Using the mapping we can derive the Hamiltonian $H = H_0 + H_{int}$, where

$$H_0 = \sum_i \left[b_z S_i^2 + b_x \sigma_i^2 + b_{xz} S_i^2 \sigma_i^2 \right] \tag{1}$$

is the most general form of the on-site term since $S^3 = S$ and $\sigma^3 = \sigma$. The sum is over all sites i. There are no odd terms by symmetry. H_{int} describes intersite interactions, characterized by energies J_{ij} which we assume decrease rapidly with distance. The b's and J's arise from effective ionic interactions. Consider a tetragonal cell with the body-center spins labeled (S_b, σ_b), and the corners labeled by coordinates $(x, y, z = 0, 1)$. The dominant interactions are between the dimerizing spin (S_b) and twisting corner spins (σ), and vice versa. Keeping these, we have

$$\begin{aligned} H_{int} = &- J_b \sum [S_b(\sigma_{000} - \sigma_{110} - \sigma_{001} + \sigma_{111}) \\ &+ \sigma_b(S_{010} - S_{100} - S_{011} + S_{101})] \end{aligned} \tag{2}$$

with $J_b > 0$. The sum is over cells. We show that the Hamiltonian $H_0 + H_{int}$ describes the phases of VO_2. The lowest interaction energy corresponds to $\sigma_{000} = -\sigma_{110} = -\sigma_{001} = \sigma_{111} = S_b$, with $S_b = 1$ or -1 in the first bracket, and similarly in the second with S and σ interchanged, which gives $E_0 = b_x + b_z + b_{xz} - 4J_b$ for the energy per site. This is the M1 phase with spins oppositely directed (antiferroelectric ordering) along the c- and the ab-diagonals. It is stable at $T = 0$ if $E_0 < 0$.

To determine the phase diagram as a function of temperature, we use a mean-field approximation. Since corners and body centers are nonequivalent, there are four order parameters: the pairs $\langle S_i \rangle$, $\langle \sigma_i \rangle$ for the corner and the body center sites, where $\langle \dots \rangle$ denotes thermal averaging. Suppose we label the spins by the sites $\mathbf{R}$ of a tetragonal lattice and a two-point basis $(\mathbf{R}, p)$, with $p = c$ for the origin (corner) and $p = b$ for the body center. Since the interaction H_{int} is antiferroelectric, the order parameters can be chosen as

$$(\langle S_{\mathbf{R}p} \rangle, \langle \sigma_{\mathbf{R}p} \rangle) = (m_{Sp}, m_{\sigma p}) e^{i \mathbf{Q}_a \cdot \mathbf{R}} \tag{3}$$

where $\mathbf{Q}_a = (\pi/a, 0, \pi/c)$, and a, c are the lattice spacings. We have solved the four coupled mean-field equations for the four order parameters numerically [25]. Going back to the original notation, we see that a body-center S_i is coupled to the nearest corner σ_j's within the same plane (A). It follows that m_{sb} is nonzero only if $m_{\sigma c}$ is nonzero, and vice versa. Thus, the group comprising body-center S spins and corner σ spins in plane A is effectively characterized by a single order parameter; we represent it by the average $m_A = (m_{sb} + m_{\sigma c})/2$. Similarly, body-center σ spins interact only with corner S spins in the B plane, forming a second group characterized by the order parameter $m_B = (m_{sc} + m_{\sigma b})/2$. Although the two groups interact through the on-site quartic term, the two order parameters can exist independently since if one is zero, the other need not be. Each describes a twist and a connected dimerization.

The M1 phase, with $m_A = m_B$, is stable at low T. If $b_{xz} = 0$, the two groups are decoupled; each is described by a (one-component) spin-1 Ising model. This well-known (Blume-Emery-Griffiths [26]) model has been used to describe He_3-He_4 mixtures and other systems. For $b_x = b_z$, the Blume-Capel phase diagram [27, 28] is reproduced. A line of second-order transitions from M1 to R phase up to $b_x/4J_b \approx 0.46$ is followed by a line

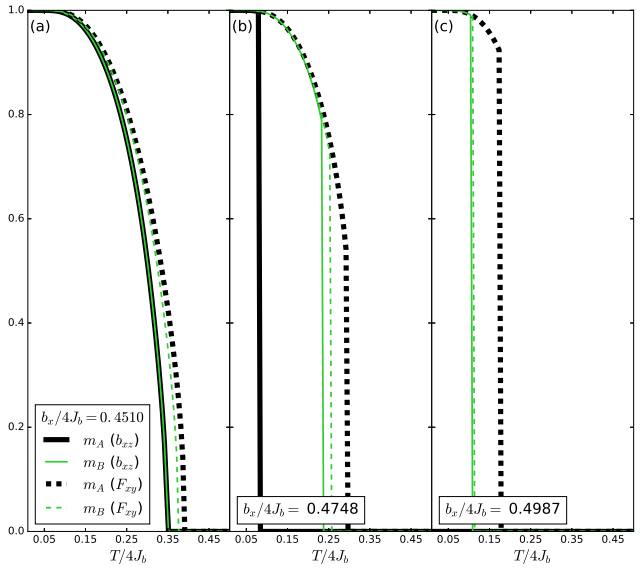

FIG. 2. Mean-field order parameter and phases. (a) Order parameters m_A and m_B including the quartic interaction b_{xz} (solid lines) or the screw axis symmetry breaking F_{xy} (dashed lines) are shown in the regime of small on-site quadratic term b_x/J_b (taking $b_z = b_x$). The M1 phase occurs at low temperature for the b_{xz} case, while the T phase develops in the F_{xy} case; a second-order transition to the R phase occurs with increasing temperature. (b) Same as in (a) but for larger on-site quadratic term. First-order transitions are present between M1, M2, and R phases (b_{xz} case) and T, M2, and R phases (F_{xy} case). (c) Same as in (b) but with further increased b_x/J_b. In the b_{xz} case, the M2 phase is present at zero temperature.

of first-order transitions up to $b_x/4J_b = 0.5$, which is important since the observed transition is first order in VO_2.

The quartic term ($b_{xz} > 0$) represents a competition between on-site twisting and dimerization. The system compromises by stabilizing the M2 phase, with $m_A \neq 0$ and $m_B = 0$ (or vice versa), between the M1 and the R phases. This is shown by the solid lines in Fig. 2 for $b_{xz}/J_b = 0.1$. There are three regimes: one with second-order transitions between M1 and R phases, one with first-order transitions between M1 and M2 and between M2 and R, and one in which the M1 phase is absent.

The M2 phase can also be stabilized by applying strain along the [110] direction [6]. This breaks the screw axis symmetry, making b_x different for corner and body sites, which we parameterize by $b_{x,corner} = (1 - F_{xy})b_x$ with $F_{xy} \ll 1$. In this case a triclinic (T) phase with $m_B < m_A \neq 0$ also appears between the M1 and M2 phases, as shown by the dashed lines in Fig. 2 where $F_{xy} = 0.03$. The transitions between T and M2 phases are second order for small b_x/J_b, and elsewhere they are first order. All of these results are qualitatively consistent with the observed phase diagram, which provides an

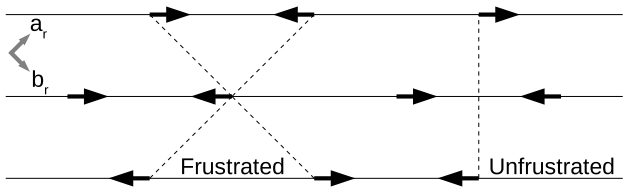

FIG. 3. Interaction between planes leading to fragile 3D order. Arrows represent the *ab*-plane (σ) degree of freedom on corner sites. 2D AFE order is established by the strong interaction between these degrees of freedom along the [110] axis, which is shown as a solid line and mediated by the body-center *c*-axis (S) degree of freedom. The interactions along this axis form the A planes as shown in Fig. 1(a). Interactions between adjacent A planes, indicated by the dashed lines on the left side, are frustrated: the 2D order within the A planes prevents this type of interaction from minimizing its energy. Weaker interaction between next-nearest-neighbor A planes, indicated by the dashed line on the right side, is required to establish 3D order. A similar situation exists for the B planes which form along the $[1\bar{1}0]$ axis.

important experimental validation of the correctness of the model. Landau free energies used in phenomenological theories [18–20] can be obtained by expanding the mean-field free energy in powers of the order parameters.

3D ordering and frustration.—The mean-field approximation (and Landau theories) may hide an important property of the Hamiltonian $H_0 + H_{int}$, which can be seen from Eq. 2 and Fig. 1. Any twisting spin σ_b interacts with only half (4) of the corner S spins which are all in *one* A plane, and the dimerizing spin S_b interacts with the 4 corner σ spins which are all in *one* B plane. In each case, the coupling with the other 4 corner spins is quartic (thus, not symmetry breaking) since the displacements are perpendicular. Therefore, the spins are divided into two groups. The body-center S- and corner σ-spins live on one set of parallel planes (A) with no quadratic (symmetry breaking) coupling between the planes. The other group, with (S, σ) interchanged, live on the perpendicular set of planes (B) and have the same property. Therefore, the Hamiltonian is invariant under the 2D global symmetry transformation: $S_i \to -S_i$, $\sigma_i \to -\sigma_i$ independently on each plane. Hence, each plane orders independently with the order parameter either m or $-m$. The ground state is 2^{2L}-fold degenerate, where L is the number of planes in each direction. These exact results remain valid in the presence of intra- and inter-plane quartic (e.g. $S_i^2\sigma_j^2$) interactions.

To see how 3D ordering may develop we need to consider other quadratic interactions which have been neglected so far, e.g., of the form $-\sum J_{ij}S_iS_j$, where S_i and S_j are in different planes. The dominant ones are again between body-centers and corners (see Fig. 1). By symmetry, all J_{ij} are the same. The interaction has the same form as Eq. 2, but with all S spins and all with

positive signs. Hence, its thermal average value in the ordered phases vanishes, irrespectively of the sign of J_{ij}. This is also true for σ spins, and for second-neighbor interactions (in the ab-planes), since quite generally, for an S_i in one plane, the S_j's in an adjacent plane add up to zero in pairs for an AFE ordered phase. Hence these interactions do not lead to 3D ordering. On the contrary, they prefer ferroelectric order *within* the planes and therefore are frustrated. This interaction is shown by the dashed lines (forming triangles) on the left side of Fig. 3.

However, interactions between spins in alternate parallel planes lead to 3D ordering, as they do not compete with the in-plane order since there is no pairwise cancellation. The strongest of these couples nearest spins on alternate planes in the perpendicular direction, and is of the form:

$$H_{3D} = -J_{3D,S} \sum S_i S_j - J_{3D,\sigma} \sum \sigma_i \sigma_j \qquad (4)$$

This interaction is shown by the dashed line on the right side of Fig. 3. It leads to 3D ordering within the set of A and/or B planes, which is ferroelectric if J_{3D} is positive, and antiferroelectric if it is negative. Since only alternate planes are coupled, each set consists of two interpenetrating subsets which are ordered independently, so that the ground state is now $2^4 = 16$-fold degenerate, corresponding to choices of $\pm m_A$ and $\pm m_B$. These results are exact. Since J_{3D} actually corresponds to third-neighbor interaction, J_{3D}/J_b is small and 3D ordering weak, and consequently each subset shows quasi 2D order.

This degeneracy is robust against two-body perturbations, as the arguments above and the (isosceles) triangular construction in Fig. 3 can be generalized to any pair of planes with arbitrary range of interaction J_{ij}. Then, the two spins forming the base of the triangle (in the second plane) are aligned if the planes are in the same subset because the base length equals an even number of lattice spacings. It is odd when the two planes are in different subsets, so that the two spins are anti-aligned, i.e, there is no ordering between the subsets in the dimerized phase. Ordering can be established (and degeneracy reduced) by making J_{ij} strong enough; but that will destroy the dimers, causing a transition to another (ferroelectric) phase.

Since the 16-fold degenerate order is protected against two-body perturbations, one may consider selective multi-body interactions which, though weaker, are allowed by symmetry. An example is $K(S_1S_2)_A(S_3S_4)_B$, where the four spins belong to four different planes, say, two body-center spins of A type and two corner spins of B type, in the most compact arrangement. For $K > 0$ this term has a lower energy when the ordering wave vectors for A and B planes are either both $\mathbf{Q}_a = (\pi/a, 0, \pi/c)$ or both $\mathbf{Q}_b = (0, \pi/a, \pi/c)$, thereby lowering the degeneracy to 8. For $K < 0$ the corresponding choice is $\mathbf{Q}_a$ for one type of plane and $\mathbf{Q}_b$ for the other.

In short, the 3D order is not only weak, it is characterized by several energy scales with different degrees of degeneracy which will appear as different crossover scales for $T > 0$. The various 3D ordering interactions have to be included to study these effects. The frustrating interactions between spins belonging to opposite (interpenetrating) subsets are generally stronger than the more distant-neighbor ordering interactions J_{3D} and the four-spin interactions K. While they do not change the degeneracy structure, their effects, which are not included in the mean-field (or Landau) theories, are important for $T > 0$ since they provide an extra source of entropy and also weaken the in-plane order. Together with the complex degeneracy including the hidden 2^{2L}-fold 2D degeneracy, they make the ordered state quite fragile and prone to breaking up into domains.

Our main results are not restricted to VO_2. The model itself applies to any rutiles, particularly to oxides of the form MO_2 (where M is a transition metal). At least five of these (M = Mo, W, Tc, α-Re, Nb) have similar low-energy paired (dimerized) structures [12–14]; all are predicted to have similar selective frustrated ordering. The materials which do not undergo the transition are also described by the model. Nor is the mechanism restricted to rutiles. For example, Ti_2O_3 (more generally, M_2O_3 [16]) with a primary corundum structure shows a transition to a monoclinic phase with similar complex paired structure [12, 15]. In this case, the pseudospin model may be different but can be derived using our template. Thus we have found a generic mechanism by which an important class of ionic crystals develop complex and fragile secondary crystalline order using selective low-dimensional pathways. The nature of the diverse electronic and magnetic states exhibited by these materials is expected to be rather different from those of usual crystals. The model provides a foundation for studying these by introducing residual electron-ion interactions [15, 19].

This research was supported by the National Science Foundation (DMR-1508680). Work in Austin was supported by the Department of Energy, Office of Basic Energy Sciences under contract DE-FG02-ER45118 and by the Welch Foundation under grant TBF1473.

[1] F. J. Morin, Phys. Rev. Lett. **3**, 34 (1959).
[2] S. Westman, Acta Chem. Scand. **15**, 217 (1961).
[3] G. J. Hyland, J. Phys. C: Solid State Phys. **1**, 189 (1968).
[4] J. B. Goodenough, J. Solid State Chem. **3**, 490 (1971).
[5] J. P. Pouget, H. Launois, T. M. Rice, P. Dernier, A. Gossard, G. Villeneuve, and P. Hagenmuller, Phys. Rev. B **10**, 1801 (1974).
[6] J. P. Pouget, H. Launois, J. P. D'Haenens, P. Merenda, and T. M. Rice, Phys. Rev. Lett. **35**, 873 (1975).
[7] J. M. Atkin, S. Berweger, E. K. Chavez, M. B. Raschke, J. Cao, W. Fan, and J. Wu,

Phys. Rev. B **85**, 020101 (2012).
[8] V. Eyert, Ann. Phys. (Leipzig) **11**, 650 (2002).
[9] Z. Yang, C. Ko, and S. Ramanathan, Annual Review of Materials Research **41**, 337 (2011).
[10] M. Nakano, K. Shibuya, D. Okuyama, T. Hatano, S. Ono, M. Kawasaki, Y. Iwasa, and Y. Tokura, Nature **487**, 459 (2012).
[11] Y. Zhou and S. Ramanathan, Proceedings of the IEEE **103**, 1289 (2015).
[12] Z. Hiroi, Progress in Solid State Chemistry **43**, 47 (2015).
[13] V. Eyert, R. Horny, K.-H. Höck, and S. Horn, Journal of Physics: Condensed Matter **12**, 4923 (2000).
[14] V. Eyert, EPL (Europhysics Letters) **58**, 851 (2002).
[15] A. Tanaka, J. Phys. Soc. Jpn. **73**, 152 (2004).
[16] M. Imada, A. Fujimori, and Y. Tokura, Rev. Mod. Phys. **70**, 1039 (1998).
[17] T. M. Rice, H. Launois, and J. P. Pouget, Phys. Rev. Lett. **73**, 3042 (1994).
[18] J. R. Brews, Phys. Rev. B **1**, 2557 (1970).
[19] D. Paquet and P. Leroux-Hugon, Phys. Rev. B **22**, 5284 (1980).
[20] A. Tselev, I. A. Lukyanchuk, I. N. Ivanov, J. D. Budai, J. Z. Tischler, E. Strelcov, A. Kolmakov, and S. V. Kalinin, Nano Letters **10**, 4409 (2010).
[21] J. Ashkin and E. Teller, Phys. Rev. **64**, 178 (1943).
[22] R. V. Ditzian, J. R. Banavar, G. S. Grest, and L. P. Kadanoff, Phys. Rev. B **22**, 2542 (1980).
[23] M. Badehdah, S. Bekhechi, A. Benyoussef, and B. Ettaki, Phys. Rev. B **59**, 6250 (1999).
[24] J. P. Santos and F. S. Barreto, Journal of Magnetism and Magnetic Materials **401**, 724 (2016).
[25] The software developed to solve the mean-field equations is available at `https://github.com/tflovorn/vo2mft` and doi:10.5281/zenodo.195417.
[26] M. Blume, V. J. Emery, and R. B. Griffiths, Phys. Rev. A **4**, 1071 (1971).
[27] M. Blume, Phys. Rev. **141**, 517 (1966).
[28] H. W. Capel, Physica **32**, 966 (1966).